scientific reports

Check for updates

OPEN

A novel *Kayvirus* species phage RuSa1 removes biofilm and lyses multiple clinical strains of methicillin resistant *Staphylococcus aureus*

Kokkarambath Vannadil Suchithra[1], Asif Hameed[1]✉, Punchappady Devasya Rekha[1], Paul Stothard[2] & Ananthapadmanabha Bhagwath Arun[1,3]✉

The emergence of methicillin-resistant *Staphylococcus aureus* (MRSA) infection is one of the global healthcare concerns. Here, we report the phenotypic and genotypic characterization of a novel multi-host *Staphylococcus* phage RuSa1, isolated from wastewater samples derived from a spotted sambar deer (*Rusa unicolor*) enclosure located at Mangalore, India. Clinical MRSA strains ($n = 18$) susceptible to RuSa1 were genetically and phenotypically diverse as determined by DNA fingerprinting and in vitro culture assays. RuSa1 displayed a latent period and burst size of 10 min and 50 PFU, respectively, and exhibited efficient biofilm removal activities against *S. aureus* ATCC BAA-44. The phage exhibited moderate UV stability (3 min) and high titre at 4–37 °C and pH 5–9. RuSa1 possessed a linear double-stranded genomic DNA with a length of 140 kb. The genome contained 30.18% GC composition and shared 82.0–94.9% sequence similarity with eleven authentic species of *Kayvirus* recognized by the International Committee on Taxonomy of Viruses based on VIRIDIC analysis. RuSa1 established distinct phyletic lineage in the maximum likelihood phylogenetic analysis of DNA encoding structural proteins and lacked genes that confer lysogeny. Based on the genotypic, phylogenetic and phenotypic data, RuSa1 is proposed to be a lytic phage and a new species of *Kayvirus* with a potential therapeutic ability against staphylococcal infections.

Keywords Bacteriophage, Multidrug resistance, *Herelleviridae*, DNA fingerprinting, Lytic phage

Staphylococcus aureus is a normal commensal of the human nasal cavity with a colonization rate of approximately 30%. It is also an opportunistic pathogen commonly found in osteoarticular, skin and soft tissue infections, and life-threatening conditions such as bacteraemia and infective endocarditis[1]. It is one of the prevalent causative agents of severe wound infections, especially in hospital settings. The colonization, persistence and the evasion of immune system in *S. aureus* is achieved by a multitude of virulence factors[2]. Even though healthy individuals raise antibodies against *Staphylococcus* antigens, some MRSA strains can breach host's adaptive immunity and cause recurrent infections[3]. Managing *S. aureus* infection is challenging due to high levels of drug resistance conferred by beta-lactamase or alteration in the drug-binding receptors. Wounds infected by MRSA are usually treated with antibiotics; however, pathogenic bacteria have developed resistance mechanisms due to overuse and misuse of these antibiotics[4]. The colonization of MRSA at the wound site disrupts the wound-healing ability of the host and increases the severity[5].

World Health Organization (WHO) has listed antimicrobial resistance (AMR) as one of the top ten healthcare concerns and predicted to claim ten million deaths per year by 2050 (WHO 2001). AMR marked its presence by the emergence of penicillin-resistant *S. aureus*, against which methicillin was developed later on. However, two years post-methicillin introduction, MRSA emerged as a global threat[6]. Vancomycin is the most common drug used to treat MRSA infections, but vancomycin-resistant strains of *S. aureus* emerged in nosocomial environment[7]. New antibiotics like cefazolin have been commercially available since 2012 and a few antibiotics

[1]Division of Microbiology and Biotechnology, Yenepoya Research Centre, Yenepoya (Deemed to be University), Deralakatte, Mangalore 575018, India. [2]Department of Agricultural, Food and Nutritional Science, University of Alberta, Edmonton, AB T6G 2P5, Canada. [3]Yenepoya Institute of Arts, Science, Commerce and Management, Kulur, Mangalore 575013, India. ✉email: asifhameed@yenepoya.edu.in; arunbhagwath@yenepoya.edu.in

are under phase III clinical trials such as dalbavancin, oritavancin and nemonoxacin to treat MRSA. The further development of resistance against these drugs by pathogenic bacteria cannot be ruled out[8]. MRSA infections prolong hospitalization and mount economic burden on patients[9].

The administration of bacteriophages to patients for therapeutic purposes is known as phage therapy[10]. Bacteriophages that can lyse and remove specific bacteria from the target site are exploited in therapy. Phages generally have a narrower-spectrum activity than antibiotics, cause a minimal effect on normal flora[9], and are safe for humans in severe staphylococcal infections such as infective endocarditis and septic shock[11]. The in vitro lytic activities of bacteriophages against MRSA have been reported[12–16]. Phage therapy was effective in treating domesticated animals[5,17] and humans[18,19]. The quest for novel phages with characteristics that are applicable to a wide range of hosts continues.

Here, we characterize *S. aureus* phage designated as RuSa1 of wild-life origin exhibiting biofilm removal and lytic activity against clinical strains of MRSA isolated from infected wounds, using standard phenotypic and genotypic assays. The genome was sequenced to gain insights into the genetic makeup and taxonomic status of RuSa1. The clinical MRSA strains susceptible to RuSa1 were characterized through DNA fingerprinting to validate the broad host range of infectivity of novel phage species.

Materials and methods

Bacterial strains and culture conditions

Staphylococcus aureus (ATCC BAA-44, ATCC 25923 and MCC 2408), *Escherichia coli* ATCC 25922, *Klebsiella pneumoniae* MCC 2716, *Streptococcus mutans* ATCC 25175 and *Enterococcus faecalis* ATCC 29212 were procured from respective culture collection centres. *Pseudomonas aeruginosa* PAO1 was from our lab repository. Other MRSA strains and coagulase-negative *Staphylococcus* were originated from patient samples.

Isolation and purification of bacteriophage

Wastewater samples were collected from a sambar deer (*Rusa unicolor*) enclosure at Pilikula Biological Park, Mangalore, Karnataka (12°55'41.5"N 74°54'01.3"E) on 16th October 2022. The sample was immediately transported to the laboratory and centrifuged (12000 ×*g*, 10 min, 4 °C). The collected supernatant was treated with 1% (v/v) chloroform to remove the residual host bacteria. The supernatant was subjected to the phage enrichment process according to Cerveny et al. (2002)[20] with minor modifications. Briefly, the sample was mixed with an equal volume of double-strength Luria Bertani (LB) broth followed by the addition of 1 ml of an overnight culture of standard as well as clinical strains of *S. aureus* with an assumption that the enrichment with multiple *S. aureus* strains enhances the possibility of isolating broad host range phages. The sample was incubated at 30 °C in a shaker incubator overnight and subjected to centrifugation (12000 ×*g*, 10 min, 4 °C). The collected supernatant was treated with 1% (v/v) chloroform to remove the remaining host bacteria (37 °C for 20 min) and to get a Bacteria-Free Filtrate (BFF).

After enrichment, the presence of phages in the sample was identified by spot assay[21]. Briefly, the *S. aureus* ATCC BAA-44 lawn made on the Muller Hinton agar plate was spot inoculated with 10 µl of BFF from the sample after final treatment with chloroform. The spot inoculated plates were incubated at 37 °C overnight under darkness. The presence of phages in the BFF was confirmed by plaque assay on double-layer agar (DLA)[22]. Serial dilutions of 100 µl of BFF were mixed with 100 µl of *S. aureus* ATCC BAA-44 overnight culture in sterile test tubes. To this, 3 ml of semisolid nutrient agar (0.6% agar) was added, mixed well, poured over precast nutrient agar plates, allowed to solidify and incubated at 37 °C overnight. Plaque-forming unit (PFU) was counted and the phage titre was determined. For purification of phage lysate, a single plaque was carefully harvested using a sterile Pasteur pipette and dissolved in phage buffer and sub cultured through plaque assay. This process was repeated thrice until uniform-sized plaques were developed[23]. The lytic activity of isolated phages was tested against six strains of *S. aureus* including three standard strains and three clinical strains by spot assay. The phage sample that showed lytic activity against the maximum number of *S. aureus* strains was processed further for purification.

RuSa1 was purified according to a previously reported protocol[24] with slight modifications. Briefly, 3 ml phage buffer was added to a completely lysed plaque assay plate and incubated at room temperature in rotation (120 rpm) for 1 h. The BFF produced by using above-mentioned protocol was transferred to a 2 ml Eppendorf tube. To this 20% (w/v) PEG 6000 was added, incubated in the ice for 1 h followed by centrifugation (20000 ×*g*, 30 min, 4 °C). The supernatant was removed to collect white pellets observed at the bottom and the tubes were centrifuged (20000 ×*g*, 20 min, 4 °C) for the complete removal of the residual PEG. To PEG precipitated phage, 200 µl phage buffer was added and mixed well followed by 200 µl 2 M KCl addition to release phages from PEG. After centrifugation (12000 ×*g*, 10 min, 4 °C), 200 µl supernatant was collected and stored at 4 °C.

Transmission electron microscopy

For electron microscopy, the high titre phage lysate (10^9 PFU/ml) was centrifuged (12000 ×*g*, 5 min, 4 °C) and 3 µl supernatant was placed onto carbon-coated copper grids and dried. After critical point drying, the grid was stained with 2% (w/v) phosphotungstic acid and observed under 200 kV (JEM-2100 plus, JEOL Japan) with 80,000 x magnification.

Determination of optimum multiplicity of infection (OMOI)

Staphylococcus aureus ATCC BAA-44 culture was infected with phage lysate with different Multiplicity Of Infection (MOI). Briefly, 1.8 ml of *S. aureus* BAA-44 culture (OD_{600} 0.2) was infected with 200 µl of phage lysate with phage titre 10^9, 10^8, 10^7, 10^6, 10^5 and 10^4 to get final MOI 10, 1, 10^{-1}, 10^{-2}, 10^{-3} and 10^{-4} ($n = 3$). The mixture was incubated at 37 °C for 5 h. After incubation, the mixture was centrifuged (12000 ×*g*, 10 min, 4 °C).

The supernatant was diluted 10-fold and a plaque assay was performed to determine the phage titre. The MOI which gave the maximum PFU was taken as OMOI[25].

One-step growth curve

The phage growth kinetic was determined by a one-step growth curve[26,27]. Briefly, 100 µl of (10^8 PFU/ml) BFF was added to 9.9 ml of *S. aureus* grown in nutrient broth (NB) with an OD_{600} of 0.5 and incubated for 5 min at 37 °C for phage adsorption (adsorption flask). After incubation, 1 ml from the adsorption flask was transferred to the new Eppendorf tube and treated with 1% (v/v) chloroform and vortexed for 10 s before being transferred to ice (adsorption control). 100 µl from the adsorption flask was added to 9.9 ml of fresh NB (A) and further diluted by transferring 1 ml to 9 ml of NB (B). At five-minute intervals, over a period of 2 h, 100 µl aliquots were taken from both A and B, mixed well with 100 µl *S. aureus* ATCC BAA-44 culture and 3 ml NB soft agar (0.6%) and plated by DLA. The adsorption control was centrifuged (10000 rpm, 10 min, 4 °C) and the supernatant was filtered through 0.2 µm syringe filter to remove adsorbed bacteria. 100 µl of the supernatant from adsorption control was mixed with 100 µl *S. aureus* ATCC BAA-44 culture and 3 ml NB soft agar (0.6%) and plated by DLA. The average number of infected cells was calculated by subtracting plaques formed in the adsorption control and average 1 (average of plaques from 0 min to the start of burst). The average burst size was calculated by dividing the average number of infected bacterial cells by an average number of released phage particles at the plateau (Average 2). Each experiment was performed in triplicates, and results are reported as mean values ± standard deviation.

$$\text{Average of infected cells} = \text{Plaque in the adsorption control} - \text{Average 1}$$

$$\text{Average Burst Size} = \frac{\text{Average of infected cells}}{\text{Average 2}}$$

Where, Average 1 = Average of plaques from 0 min to the start of the burst.
Average 2 = Average of released phage particles at the plateau.

Phage resistance frequency

To determine the phage resistance frequency, *S. aureus* ATCC BAA-44 culture (OD_{600}, 0.2) was diluted to 1:100 in NB. 100 µl of diluted *S. aureus* ATCC BAA-44 culture and 20 µl of phage lysate with titre 10^8 were mixed in a test tube and incubated for 10 min for phage adsorption. To this, 3 ml semisolid NA (0.6%) was added, mixed well and immediately poured onto the NA plate, allowed to solidify and incubated at 37 °C overnight. Bacteriophage-insensitive mutants were counted at 24 and 48 h intervals. The phage resistance frequency was calculated by dividing the number of bacteriophage-insensitive mutants and the initial CFU of the *S. aureus* ATCC BAA-44[28].

Growth Inhibition assay

A bacterial growth inhibition assay was performed according to a previously described method[29]. Briefly, 180 µl of bacterial culture in NB (OD_{600}, 0.2) was mixed with 20 µl of 10^9, 10^8 and 10^7 PFU/ml of phage lysate to obtain different MOIs such as 10, 1 and 0.1, respectively, in 96-well microplate. Phage-free controls were treated with the phage buffer alone. Plates were incubated at 37 °C for 8 h, and the bacterial growth was monitored by OD_{600}. To check the inhibition after 24 h incubations, the starting culture (OD_{600}, 0.2) was diluted 1:100 and repeated the same pattern as discussed above for an 8 h kinetic assay. The microplates were incubated at 37 °C without shaking for 24 h. The final absorbance at the OD_{600} was measured using a plate reader.

Phage stability assay

To check the stability of RuSa1, the phage lysate with a known titre was exposed to different temperatures and pH for 6 h. The phage titre was determined after the exposure by plaque assay as described above. The lysate was exposed to UV-C radiation in the biosafety cabinet with a wavelength of 254 nm and an intensity of 40 µW/cm^2 for 10 min. Aliquots were retrieved every minute to check the viability by spot and plaque assays.

Culture coupled with fluorescence imaging and phenol red testing

The *S. aureus* ATCC BAA-44 culture (OD 0.2, 180 µl) was treated with RuSa1 (20 µl, 10^8–10^9 PFU ml^{-1}) in 96-well microplates to get final MOIs of 10 and 1, and incubated at 37 °C under static conditions in darkness. Optical density (OD) readings were taken after 6 h of incubation (OD_{600}). Phenol red indicator (1%, w/v) was added to all the wells and absorbance was read at 450 and 560 nm for measuring acidity and alkalinity, respectively. Cells were harvested (10000 rpm, 5 min, 4 °C), washed twice in phosphate-buffered saline (PBS) and resuspended in 200 µl of acridine orange/ethidium bromide (AO: EtBr, 1:1, v/v) followed by incubation at 37 °C for 1 h under darkness. Cells suspension was subjected to centrifugation (12000 ×*g*, 10 min, 4 °C) to remove the stain, washed twice in PBS and observed under a fluorescent microscope (100 x magnification).

Anti-biofilm assay

Staphylococcus aureus ATCC BAA-44 was treated with RuSa1 in a 96-well (MOIs 10, 1, 10^{-1}) plate for biofilm quantification. The initial OD_{600} was set to 0.5 for the assay. After a 24-hour incubation at 37 °C in static conditions, the planktonic cells were discarded, and the adherent biofilm was washed with PBS before being fixed with 95% methanol for 10 min. The fixed biofilm matrix was stained with crystal violet % (w/v) for 10 min, followed by a PBS wash to eliminate any excess stain. The stained biofilm cells were then solubilized using 33% acetic acid and quantified at OD_{585}[30–32]. The percentage of biofilm inhibition was calculated by comparing the

results to the phage-free *S. aureus* control. For biofilm imaging, *S. aureus* ATCC BAA-44 was treated with RuSa1 in a 24-well plate with MOI 10 and 1. After overnight incubation, biofilms formed in 24-well plates were washed with sterile PBS, mixed with a mixture of AO: EtBr (1:1, v/v) and incubated at room temperature under darkness for 15 min followed by fluorescence microscopy (Zoe).

Biofilm disruption assay was performed according to Kabwe et al. (2020)[33] with the following modifications. Preformed biofilm (18 h old) of *S. aureus* ATCC BAA-44 in a 96-well microplate was treated with varying titre (10^4–10^8 PFU ml^{-1}) of RuSa1 and incubated at 37 °C for 6 h. Plain phage buffer was added to the control wells. Residual biofilm was quantified using the crystal violet (0.1%, w/v) staining method as described above[30,31].

Antibiotic susceptibility testing

Antibiotics of class beta-lactams (oxacillin, 1 µg), tetracyclines (tetracycline, 30 µg), lincomycins (clindamycin, 2 µg), sulfonamides (co-trimoxazole, 25 µg), aminoglycosides (gentamicin, 10 µg) and glycopeptides (vancomycin 30 µg) were tested on wound isolates of *S. aureus* using Kirby Bauer disc diffusion method. *S. aureus* ATCC 25,923 served as a control strain. The *S. aureus* culture (200 µl; OD_{600}, 0.5) was swabbed onto MHA plates. Antibiotic discs (HiMedia) were placed on the swabbed culture and gently pressed. The plates were incubated for 18 h at 37 °C, followed by measurement of zones of inhibition and each strain was determined as resistant or sensitive according to the chart provided by the manufacturer. Strains exhibiting resistance to oxacillin and three or more antibiotics were considered MRSA and MDR, respectively.

Genotyping of bacterial hosts

Genetic similarity between the clinical isolates of *S. aureus* susceptible to RuSa1 was tested using BOX PCR. The DNA of all the 20 clinical strains of *S. aureus* were extracted by phenol-chloroform method[34] and subjected to BOX PCR using BOX A1R (5 CTACGGCAAGGCGACGCTGACG-3) according to[35]. Twenty-five µl reaction mixture was prepared to have a master mixture of 12 µl, 1 µl primer, and 5 µl of DNA template and molecular grade water. PCR condition involves initial denaturation at 94 °C for 5 min, followed by denaturation at 94 °C for 1 min, annealing at 40 °C for 2 min, extension at 72 °C for 2 min (35 cycles), and a final extension at 72 °C for 10 min. The dendrogram was constructed using an unweighted pair group method with UPGMA[36].

Host range determination

The lytic activity of RuSa1 was tested against Gram-negative and Gram-positive organisms, which include *S. aureus* (ATCC BAA-44, ATCC 25923, MCC 2408), two clinical coagulase-negative *Staphylococcus*, *P. aeruginosa* PAO1, *E. coli* ATCC 25922, *K. pneumoniae* MCC 2716, *Streptococcus mutans* ATCC 25175 and *E. faecalis* ATCC 29212 by spot assay using different dilutions of phage lysate followed by confirmation with plaque assay (DLA method). Lytic activity of RuSa1 was tested ($n = 3$) on 20 clinical strains of MRSA isolated from wound infections of patients admitted to Yenepoya Medical College Hospital by performing spot assay, plaque assay and growth inhibition assay.

Phage lysogeny test

Phage lysogeny were determined according to Altamirano et al. (2021)[37]. Briefly, the DLA spot assay was performed on the lawn of *S. aureus* ATCC BAA-44 using different dilutions of the phage. Plates were incubated at 37 °C for 96 h and the phage-resistant mutants were picked up and streaked over a nutrient agar (A) to get individual colonies and incubated at 37 °C overnight. The next day, 100 µl of the *S. aureus* ATCC BAA-44 at OD_{600} 0.5 was mixed with 3 ml of semi-solid agar and poured over a solidified nutrient agar plate (B) and allowed to solidify. The colonies from plate A were inoculated at various spots onto plate B, incubated at 37 °C for 4 days and checked daily for signs of lysis. The tests were conducted in triplicates.

Phage genomic DNA isolation

Genomic DNA was extracted from 200 µl PEG precipitated lysate by phenol-chloroform method with slight modifications[32,38]. Briefly, the lysate was treated with 2 µl of proteinase K and 0.1 M EDTA and incubated at 56 °C for 90 min. After incubation, an equal volume of buffered phenol (10 mM Tris, 1 mM EDTA) was added and tubes were mixed gently, followed by centrifugation (12000 ×*g*, 2 min, 4 °C) to collect an aqueous layer. After that added 200 µl of chloroform and centrifuged was carried out at 10,000 × *g* for 2 min, and an aqueous layer was collected. Twenty microliters of 3 M sodium acetate (pH 4.8) and 400 µl of molecular-grade absolute ethanol were added to it and DNA was pelleted by centrifugation (10,000 × *g*, 10 min) followed by washing in 70% ethanol. The pellet was allowed to dry at room temperature and then resuspended in 30 µl of nuclease-free water. The purified genomic DNA was assessed qualitatively and quantitatively by the combined application of agarose gel electrophoresis and Colibri (LB 915).

Whole genome sequencing and phylogeny

The genome was sequenced on an Illumina Miseq using 500-cycle paired-end chemistry. A de novo de-Bruijn graph-based assembly was carried out by Spades[39]. The quality of genome assembly was assessed by the Quast tool[40]. The genome was annotated by BV-BRC[41] and HHpred[42] and visualized through Proksee[43]. Comparative genomic analysis were carried out using BLAST tool[44] of Proksee and Virus Intergenomic Distance Calculator (VIRIDIC)[45]. Nucleotide sequences of interest were retrieved from NCBI and aligned through Clustal X[46]. Phylogenetic reconstructions were made through MEGA5[47] using maximum-likelihood algorithm[48]. Tree topology was evaluated by bootstrap resampling after 1,000 replications[49].

Statistical analysis

Statistical significance (*$P<0.1$, **$P<0.05$, ***$P<0.01$, ****$P<0.0001$) was measured using one-way analysis of variance (ANOVA) with Tukey's multiple comparisons test using GraphPad Prism.

Results and discussion

RuSa1 is a broad host-range phage infecting *Staphylococcus aureus*

After an extensive screening of wastewater resources in and around Mangalore (~35 samples of environmental and clinical origin), phages infecting multiple strains of *S. aureus* were isolated from the enrichment culture of the wastewater sample derived from a sambar deer (*R. unicolor*) enclosure at Pilikula Biological Park, Mangalore. We used multiple strains of MRSA for sample enrichment. The spot assay revealed lytic activity of phages against *S. aureus* ATCC BAA-44 (Fig. 1a), which was confirmed by DLA plaque assay (Fig. 1b). Since DLA showed PFUs of different morphology, plaques were further purified to yield a uniform PFU (1 mm) on DLA plates. Spot assay

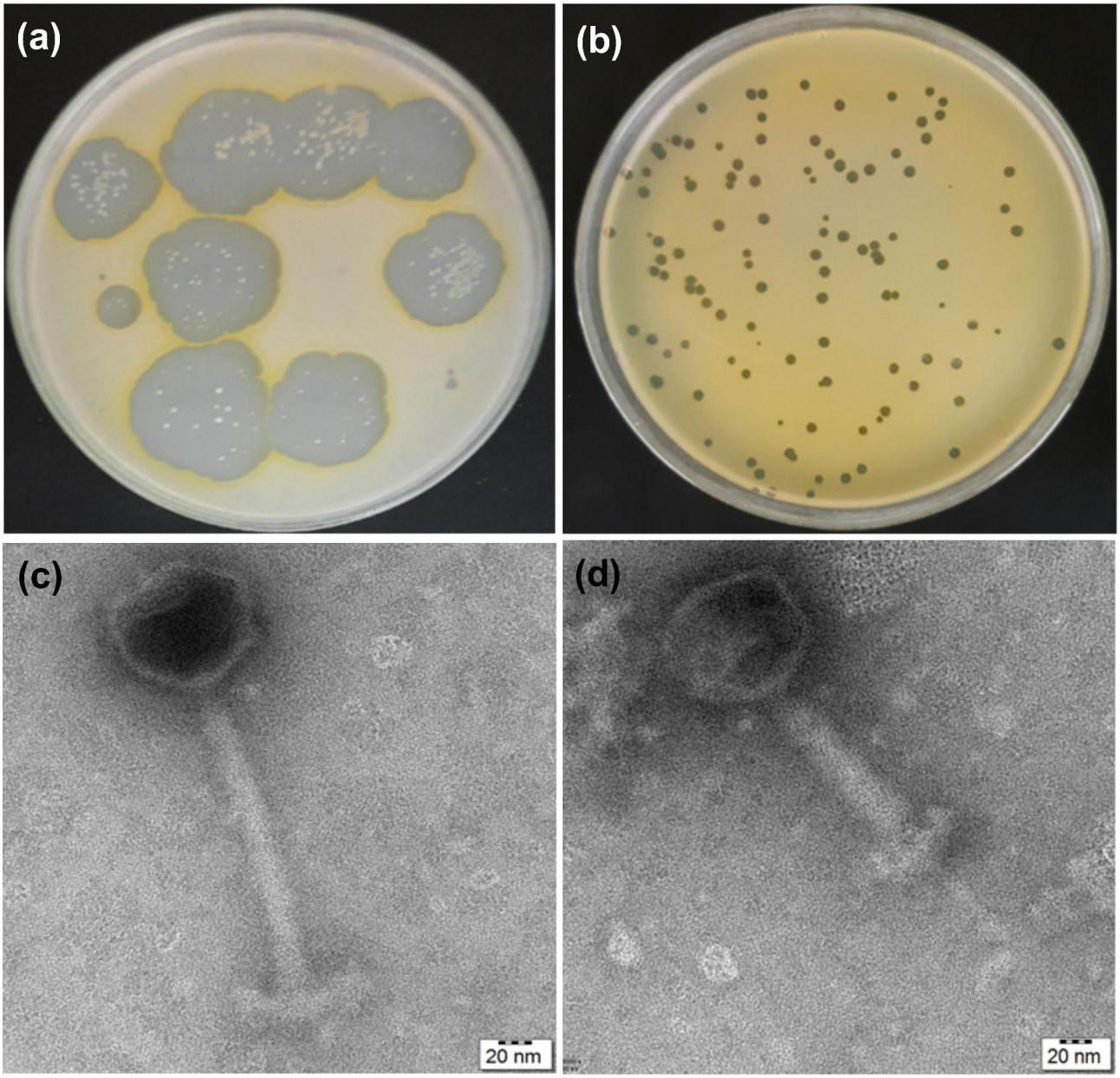

Fig. 1. Isolation and purification of *Staphylococcus* phage RuSa1 from the wastewater sample. Spot assay showing lytic activity of crude phage extract (**a**). Plaque assay showing a mixed culture of phages in crude extract (**b**). Transmission electron microscopic images of RuSa1; scale bar, 20 nm (**c**, **d**); Culture tests were performed on the lawn of *S. aureus* ATCC BAA-44 and plates were incubated at 37 °C overnight under darkness. Culture tests were performed on the lawn of *S. aureus* ATCC BAA-44 and plates were incubated at 37 °C overnight under darkness.

confirmed the lytic activity of RuSa1 on *S. aureus* ATCC BAA-44. Earlier, phages infecting multiple clinical strains of *S. aureus* were isolated from the samples associated with domesticated animals such as pig[50], cow[51] and goat[52]. This is the first report of a phage of wildlife origin infecting *S. aureus* in India.

The purified phage isolates exhibited smaller plaque sizes indicating bigger head sizes[53]. To verify this assumption and gain more insights into morphological features, transmission electron microscopy (TEM) was carried out for RuSa1. TEM showed an icosahedral head of RuSa1 having a diameter of 70–80 nm, a contractile tail (160–165 nm) and a terminal base plate (18–20 nm) (Fig. 1c,d). The morphology of RuSa1 was in line with phage *Staphylococcus* phage Stab20 in general and *myoviruses* in particular[54].

RuSa1 inhibited *Staphylococcus aureus* ATCC BAA-44 at low MOIs

RuSa1 exhibited a high phage titre at MOI 1 and 0.1 ($P < 0.0001$), whereas the phage titre was found significantly low at MOIs of $< 10^{-3}$ (Fig. 2a). The one-step growth curve of RuSa1 indicated that it has a very short latency of 10 min and burst size of 50 phages per bacteria (Fig. 2b). The latent period of RuSa1 is lower than the other members of the reported *Kayvirus*. Cessation of *S. aureus* ATCC BAA-44 growth was recorded in the presence of high MOI of RuSa1, whereas the bacterial growth was gradually decreased in lower MOIs (Fig. 2c). Significant ($P < 0.0001$) growth inhibition was found in all tested MOIs as evident through 24 h data (Fig. 2d).

The emergence of phage-resistant mutants is one of the concerns in phage therapy. The pathogenic bacteria might evolve rapidly against the phages hence making it useless for the therapy. The phage resistance frequency of RuSa1 was 3.7×10^{-7} CFU/ml and 1.4×10^{-7} CFU/ml after 24 and 48 h, respectively (Fig. 2e,f), which was lower than the frequency of known staphylococcal phages[28].

Temperate phages frequently integrate their DNA into the host cells hence could potentially transfer genes involved in virulence, toxin production and antibiotic resistance, etc. making the hosts more virulent (lysogenized host) by the process called lysogenic conversion[37]. RuSa1 lacked lysogenic properties as the phage-resistant mutants failed to lyse the lawn of host bacteria (*S. aureus* ATCC BAA-44) during the lysogenicity test (Fig. 2g,h). Colonies that are positive for lysogenic test and likely harbouring the prophage will show signs of lysis, such as plaques, halos, or a loss of turbidity on the surrounding lawn, resulting from the spontaneous release of the phage[37]. The mutant strains that emerged at 48 and 72 h lacked lytic activity against *S. aureus*. As all the screened colonies showed a negative result in the lysogeny test, it can be concluded RuSa1 is strictly lytic. The lysogenicity test, which is based on the principle of spontaneous release of phage particles from the lysogenised host, provided no evidence for the possible lysogenic conversion of the host by RuSa1. Thus, RuSa1 could be a potential candidate for phage therapy as it most likely eliminates target bacteria before cell replication.

Thermal, pH and UV stability of RuSa1

High phage titre was obtained when RuSa1 was treated at 4–37 °C, whereas phage titre declined significantly at ≥ 50 °C (59.8%, $P < 0.0001$) (Fig. 3a). Similarly, high phage tire was recorded when phages were treated with

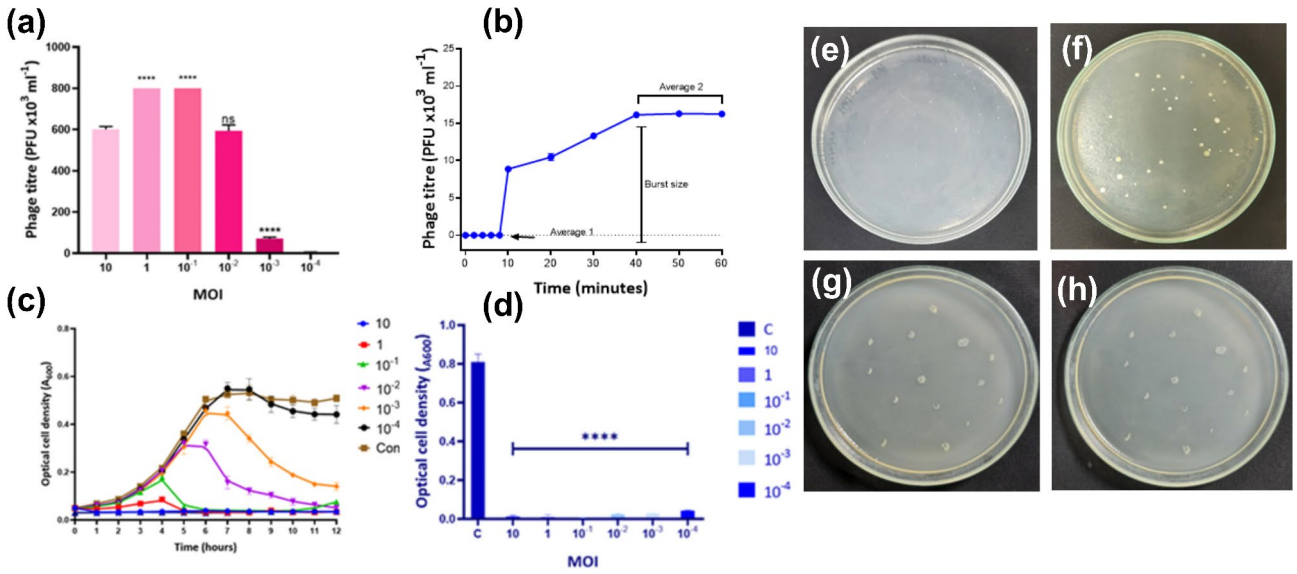

Fig. 2. Determination of MOIs, latency, bust size, and infection of *Staphylococcus* phage RuSa1 on *S. aureus* ATCC BAA-44. Optimum MOI (**a**), one step growth curve (**b**) and impact of different MOIs of RuSa1 on growth of *S. aureus* ATCC BAA-44 (**c**) are shown. Bar diagram shows the impact of various MOIs of RuSa1 on the growth of *S. aureus* ATCC BAA-44 after 24 h incubation (**d**); phage-free ATCC BAA-44 served as a control. DLA plate showing the frequency of development of phage-resistant mutants after 24 h (**e**) and 48 h of incubation (**f**). Lysogeny test showing the non-lytic activity of phage resistant mutants after 24 h incubation (**g**) and 96 h of incubation (**h**). Statistical significance was determined using One-way ANOVA after Tukey's multiple comparisons test. Error bar, mean ± SD ($n = 3$). *$P < 0.1$, **$P < 0.05$, ***$P < 0.01$, ****$P < 0.0001$; ns, non-significant.

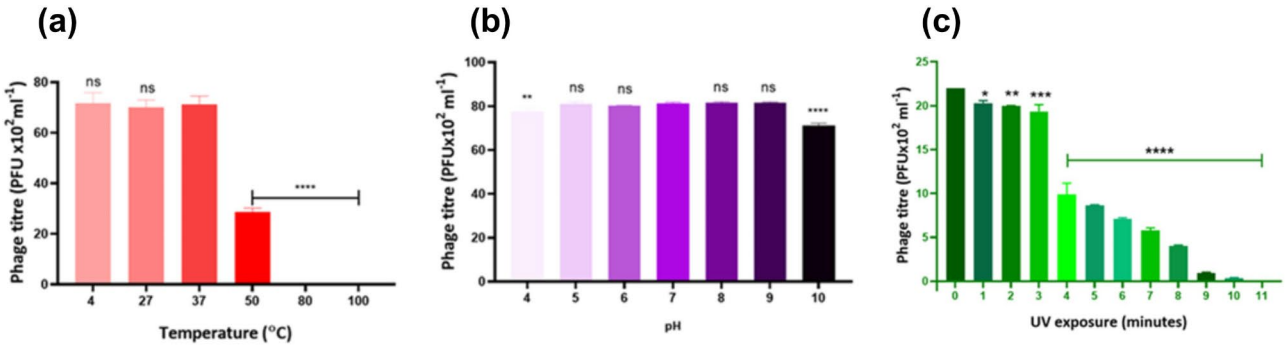

Fig. 3. Stability assay for *Staphylococcus* phage RuSa1. Impacts of temperature (**a**), pH (**b**) and UV irradiation (**c**) on the infectivity of RuSa1. Tests were performed on the lawn of *S. aureus* ATCC BAA-44. Samples incubated at 37 °C and pH 7 were used as controls in (**a**) and (**b**), respectively; samples without UV exposure served as control in (**c**). Statistical significance was determined using one-way ANOVA after Tukey's multiple comparisons test. Error bar, mean ± SD ($n = 3$). *$P < 0.1$, **$P < 0.05$, ***$P < 0.01$, ****$P < 0.0001$; ns, non-significant.

pH 5–9, whereas phage titre declined significantly after pH 4 (3.21%, $P < 0.05$) and pH 10 (11.53%, $P < 0.0001$) treatments when compared to pH 7 control (Fig. 3b). Phage titre gradually declined with the duration of UV illumination and exposure for > 10 min was lethal to RuSa1 (Fig. 3c). RuSa1 showed a shelf life of 60 days when maintained at room temperature (25 °C).

RuSa1 displays strong anti-biofilm properties

The bacterial growth was inhibited significantly (99%, $P < 0.0001$) by RuSa1 as compared to the phage-free control in liquid culture (Fig. 4a). Fluorescence microscopy substantiated the declined cell number due to RuSa1 as compared to phage-free control (Fig. 4b,c). Although RuSa1 infection did not significantly alter the media alkalinity, it significantly (41%, $P < 0.0001$) hampered media acidification as compared to phage-free control (Fig. 4d,e). Media acidification is mostly due to fermentative bacterial organic acid secretion. This differential chromogenic property could be exploited in the selective detection of *S. aureus* using RuSa1.

We further investigated the antibiofilm activities of RuSa1 on *S. aureus* ATCC BAA-44. While MOI 10 (10^8 PFU/ml) and 1 (10^7 PFU/ml) were found to be lethal to biofilm formation, significant (> 88%, $P < 0.0001$) inhibition of biofilm formation was observed under lower MOIs of RuSa1 (Fig. 5a). Fluorescence microscopy substantiated a strong antibiofilm activity of RuSa1 at MOIs 10 and 1 as compared to phage-free cell control (Fig. 5b). There was significant disruption of pre-established biofilm at the wells treated with 10^8 PFU/ml RuSa1 (76%, $P < 0.0001$), whereas 10^7 and 10^6 PFU/ml showed 25% and 13% disruption, respectively (Fig. 5c). Antibiofilm activities of RuSa1 was in line with the *Kayvirus* phenotype[55].

RuSa1 inhibits multiple clinical MRSA isolates

We employed *S. aureus* ATCC BAA-44, an Iberian clone of MRSA isolated from hospital[56,57], as a standard host bacterium for characterizing RuSa1. The ability of RuSa1 to infect multiple strains was assessed using clinical strains of MRSA ($n = 20$). All clinical strains were resistant to oxacillin confirming that they are MRSA (Table S1). While three tested strains were sensitive to multiple classes of antibiotics (Fig. 6a), seventeen strains exhibited resistance (Fig. 6b). We found five different clusters for MRSA as determined using BOX PCR (Fig. 6c). RuSa1 was found to lyse 18 strains of the tested MRSA strains (Fig. 6d, Fig. S1a–e). Even though spot assay and plaque assay showed negative lytic activity of RuSa1 on MRSA clinical strains M10 and M12, a slight reduction in the growth was observed for both in the growth inhibition assay compared to the control. In contrast, RuSa1 failed to lyse *P. aeruginosa* PAO1, *E. coli* ATCC 25922, *K. pneumoniae* MCC2716, *S. mutans* ATCC 25175, *Enterococcus faecalis* ATCC 29212 and two clinical isolates of coagulase-negative *Staphylococcus* from our lab isolates in spot assay and plaque assay. The specificity of phages is reportedly due to their selective interactions with host cell receptors through tail fibre protein[58], which is restricted sometimes to particular species/strain[59]. However, few phages can lyse multiple bacterial hosts and hence categorized as broad host range phages. The selection of these phages enhances the success of phage therapy[60]. Our data not only substantiated the genetic heterogeneity of MRSA, but also provided evidence for the broad host range of the new *Staphylococcus* phage RuSa1.

RuSa1 is a novel species of *Kayvirus*

RuSa1 harbored double-stranded linear DNA with 141,098 bp having GC content 30.18 mol%. It had 249 coding regions and 4 tRNAs; among the CDSs, 75 codes for proteins with known functions and others were hypothetical proteins as determined through BV-BRC[41] or HHPred[42]. The circular map displaying salient genomic features of RuSa1 are shown in Fig. 7a. The topmost hits obtained during genome BlastN of RuSa1 are summarized in Table S2. Unclassified *Staphylococcus* phage Stab20 (96.54%, query coverage 95%) was the topmost hit followed by *Staphylococcus* phage S3 (98.75%, query coverage 94%). In addition, the high pairwise similarity was recorded between RuSa1 and *Staphylococcus* phages vB_SauH_IME522, VB_SavM_JYL01, VB-SavM-JYL02 and vB_ScoM-PSC1, which were affiliated to *Kayvirus P108*, subfamily *Twortvirinae*, and family *Herelleviridae*. *Kayvirus*

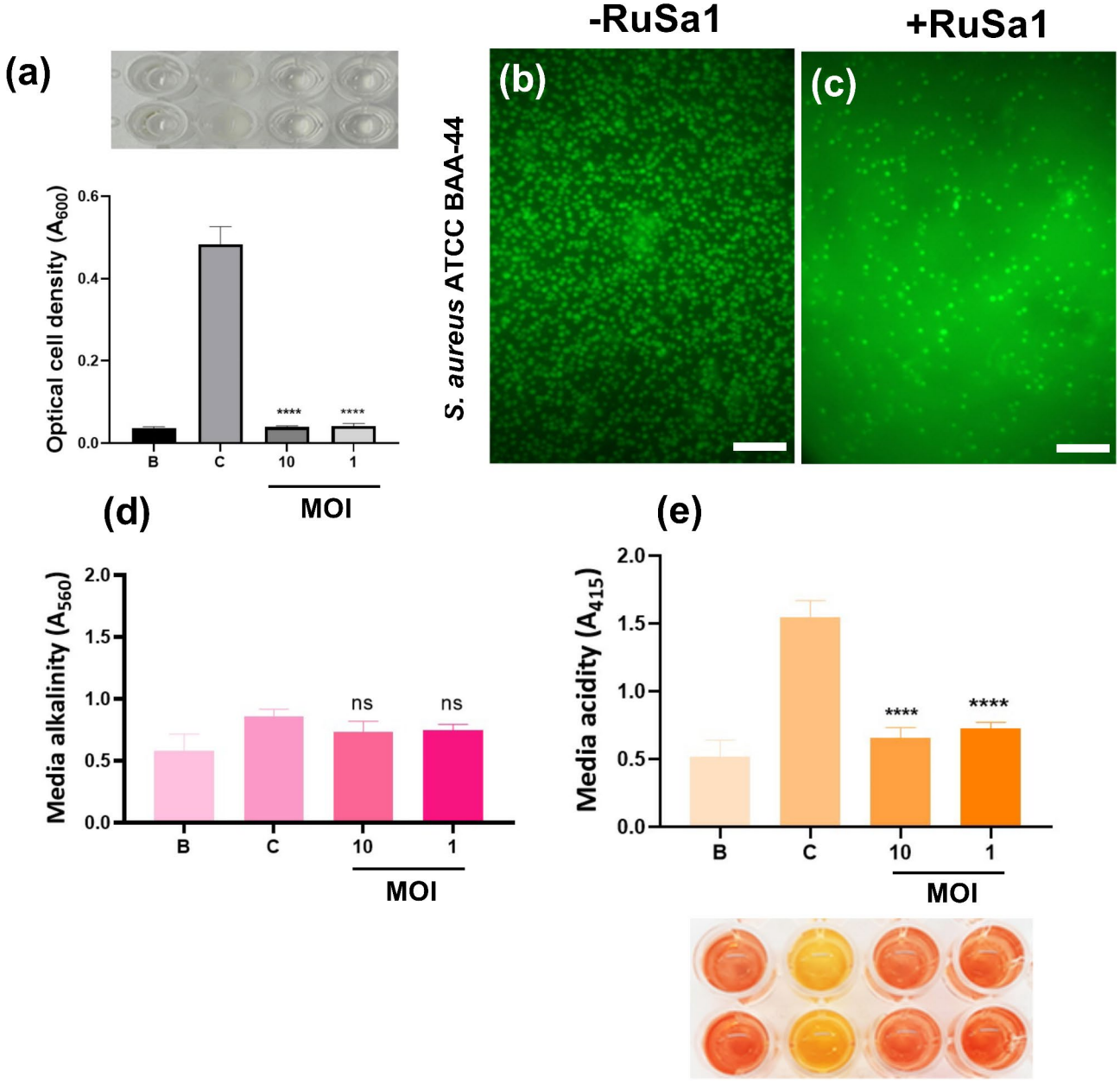

Fig. 4. Impact of *Staphylococcus* phage RuSa1 on liquid cultures of *S. aureus* ATCC BAA-44 growth and associated variation in media pH. Bacterial cell growth inhibition by RuSa1 at MOI 10 and 1 (**a**); phage-free cells served as control (C); inset: a portion of microplate revealing visible variation in *S. aureus* ATCC BAA-44 turbidity. Fluorescent image shows the bacterial cell growth in the absence (**b**) and presence of RuSa1 (**c**) Scale bar, 100 µm. The changes in culture media alkalinity (**d**) and acidity (**e**) due to phage infection are shown. Inset: a portion of the microplate showing the visible changes in color after the addition of the phenol red. Error bar, mean ± SD ($n = 3$); *$P < 0.1$, **$P < 0.05$, ***$P < 0.01$, ****$P < 0.0001$; ns, non-significant.

is the taxon specifically infecting *Staphylococcus* and constitutes the dominant portion of therapeutic phages against *S. aureus*[54,61–63] RuSa1 was found to be closely related to *Kayvirus P108* and unclassified *Staphylococcus* phages Stab20 and S2.

The genus *Kayvirus* currently accommodates eleven species according to the International Committee on Taxonomy of Viruses (ICTV). We employed VIRIDIC to calculate the genomic sequence similarity between RuSa1 with established species of *Kayvirus* as well as stab20. RuSa1 shared the highest genomic sequence similarity to *Kayvirus P108* (94.9%) while < 94.9% similarities were recorded for other authentic *Kayvirus* species ($n = 10$) enlisted by ICTV (Fig. 7b). The genus and species cluster table produced by VIRIDIC analysis authenticate the novel species status of RuSa1 (Table S5). A comparative map of RuSa1 with authentic *Kayvirus P108* is shown in Fig. S2 and a map additionally containing *Staphylococcus* phage Stab20 is depicted in Fig. S3.

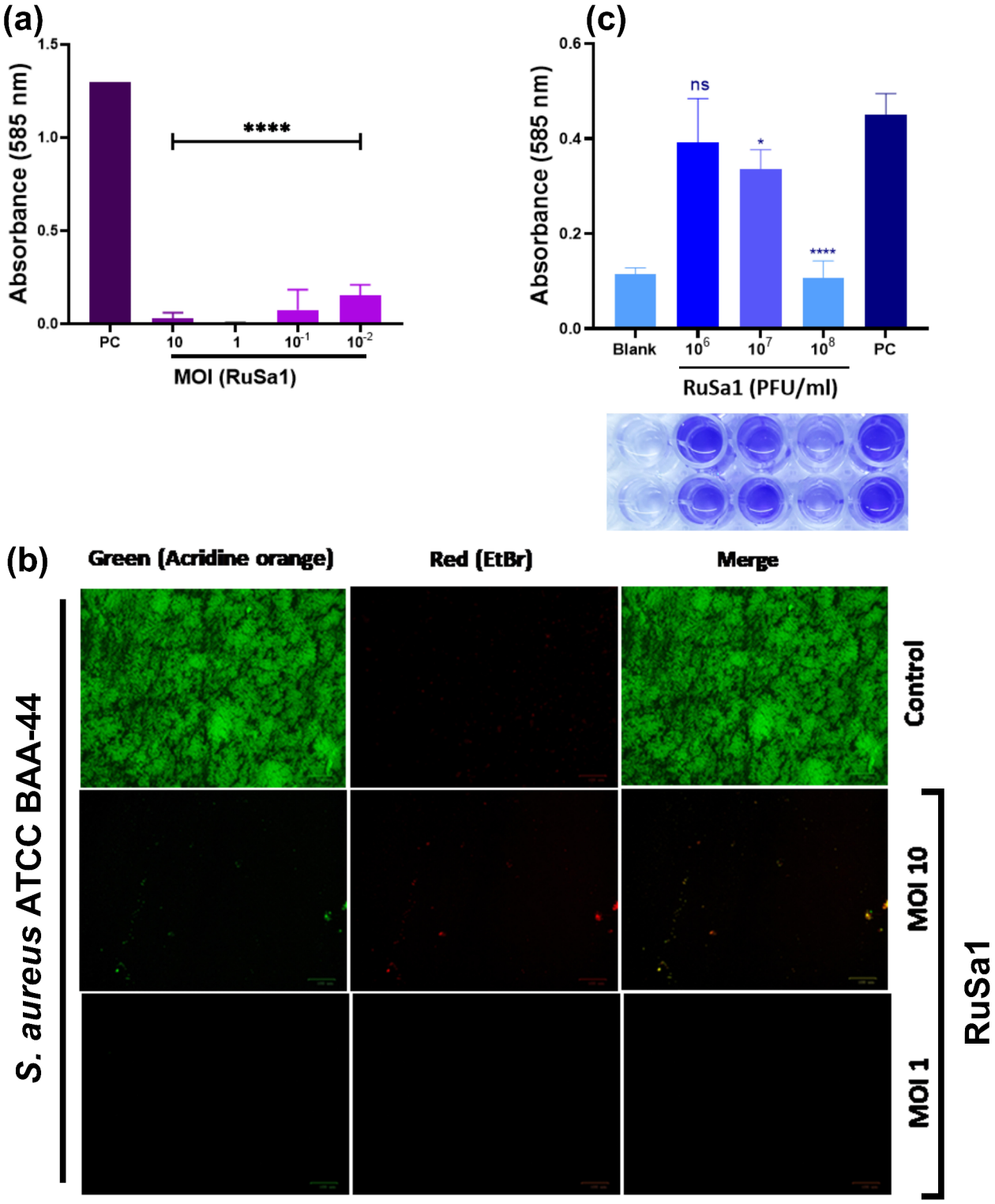

Fig. 5. Anti-biofilm activity of *Staphylococcus* phage RuSa1. The bar graph shows the biofilm quantification of *S. aureus* ATCC BAA-44 in the presence of Rusa1 (**a**). Fluorescent microscopy of *S. aureus* ATCC BAA-44 biofilms stained with acridine orange and ethidium bromide (**b**). Phage-free *S. aureus* ATCC BAA-44 served as a control; scale bar, 100 µm. The bar graph shows the quantification of residual biofilm of S. *aureus* ATCC BAA-44 as a function of Rusa1 infection (**c**); inset, residual crystal violet.

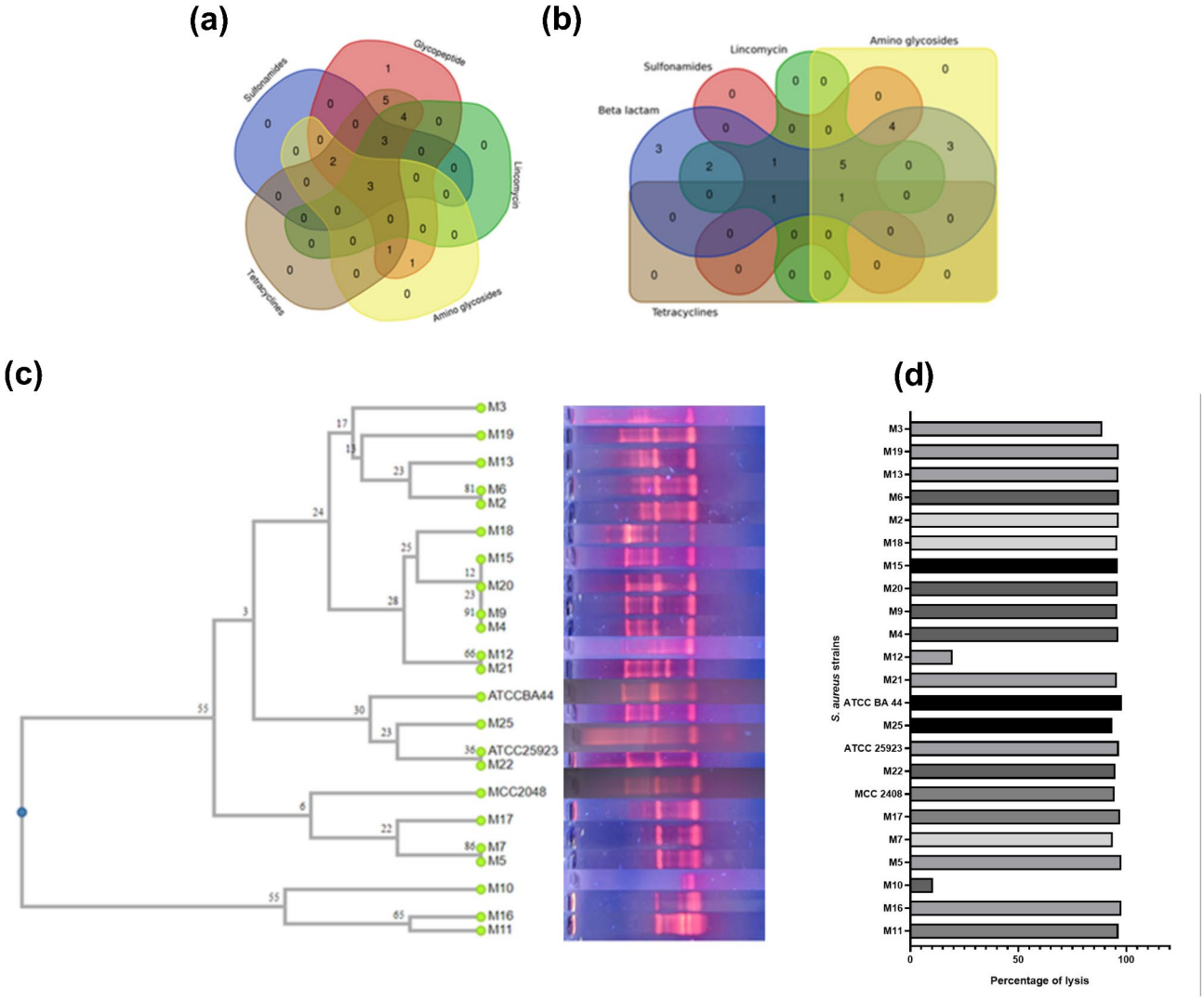

Fig. 6. Antibiotic assay and BOX PCR genotyping of *S. aureus* strains susceptible for *Staphylococcus* phage RuSa1. Venn's diagram shows the sensitivity (**a**) and resistance (**b**) patterns of different clinical isolates of *S. aureus* to the tested antibiotics. Dendrogram generated for the BOX PCR amplicons visualized on agarose gel obtained for clinical MRSA and standard strains of *S. aureus* (ATCC 25923, MCC 2048, ATCC BAA-41) created using DendroUPGMA[65] (**c**). The percentage lysis of MRSA isolates achieved due to RuSa1 infection is shown (**d**); please see Supplementary Fig. S1a–e for time-course analysis.

The nucleotide sequence of genes encoding tail protein (WEU67665), tail sheath (WEU67498) and baseplate wedge subunit (WEU67514) of RuSa1 were subjected to maximum likelihood phylogenetic analysis based on the Tamura and Nei model. RuSa1 formed distinct phyletic lineages associated with the clade that accommodate *Kayvirus P108* during the phylogenetic reconstruction of tail protein (Fig. S4), tail sheath (Fig. S5) and baseplate wedge subunit (Fig. S6). The taxonomic uniqueness of RuSa1 and its phylogenetic neighborhood with *Kayvirus P108* were further substantiated by the strong bootstrap confidence of the nodes (92–100%) obtained during the phylogeny of the tail sheath and baseplate wedge subunit. Interestingly, *Staphylococcus* phage Stab20 formed a separate lineage (>99% bootstrap support) distantly associated with the clade that accommodated both RuSa1 and *Kayvirus P108* suggesting its taxonomic novelty; however, additional experiments are needed to validate this notion. While phenotypic data distinguished RuSa1 from other related *Kayviruses* (Table S4), the VIRIDIC heatmap and the maximum likelihood phylogeny of tested gene sequences provided genetic distinction for RuSa1. Furthermore, the absence of gene encoding integrase corroborated the non-lysogenic phenotype of RuSa1. According to the new virus classification system of ICTV[64], *Staphylococcus* phage RuSa1 merits a new species status within the genus *Kayvirus*, which typically harbors phages active against *S. aureus*.

Conclusion

The morphological, physiological, phenotypic, genotypic and phylogenetic data substantiated *Staphylococcus* phage RuSa1 as a new lytic phage species affiliated with the genus *Kayvirus* and family *Herelleviridae*. RuSa1 exhibited strong antibiofilm and cell killing activities against genetically diverse MRSA that have been isolated

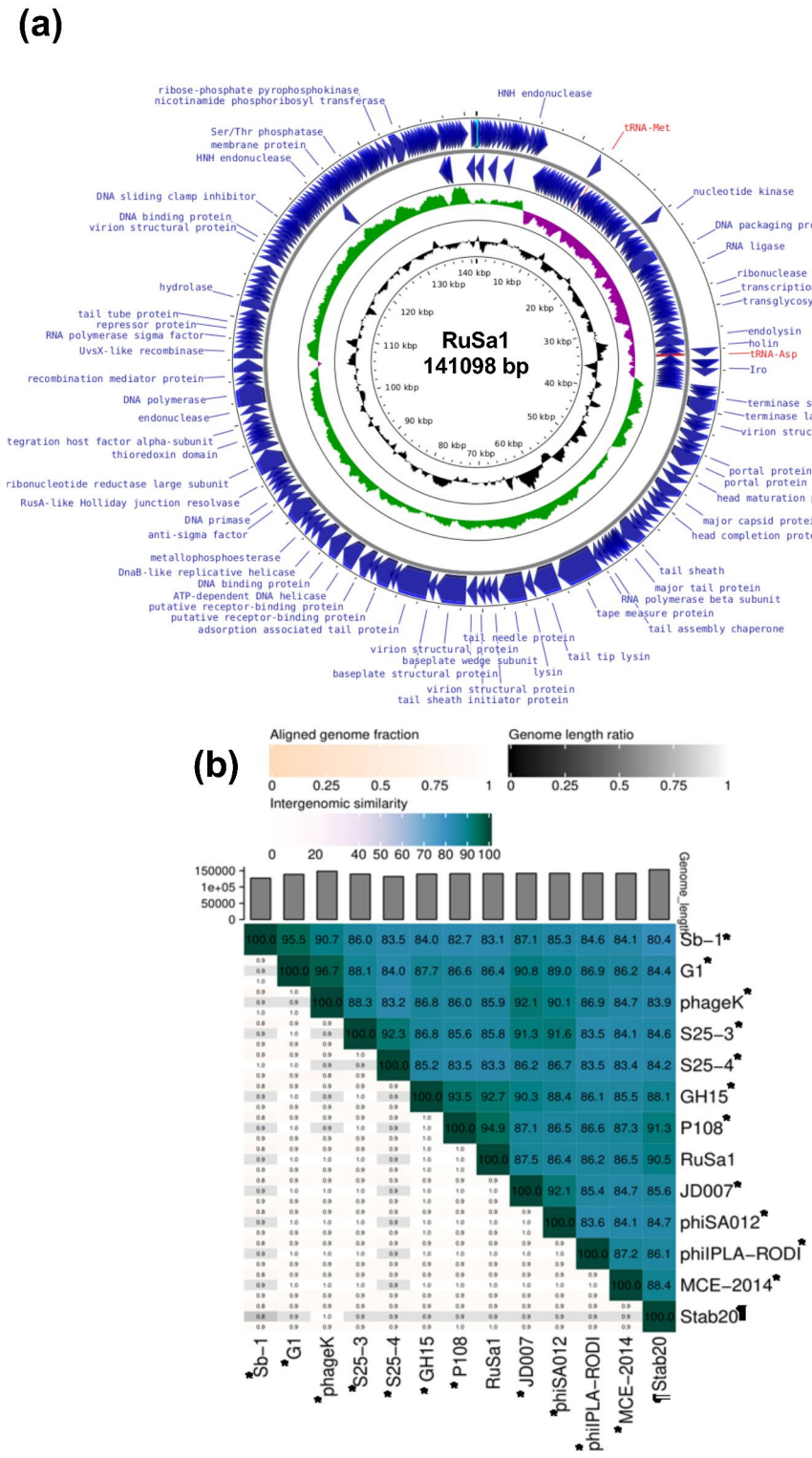

Fig. 7. Circular plot showing the genomic features of *Staphylococcus* phage RuSa1 (**a**). The genome harbored 141,098 bp. The plot was generated and annotated through Proksee[43]. Heat map of pairwise intergenomic distances/similarities amongst the newly isolated (RuSa1) and related *Kayvirus* representatives. Genomic distance matrix was calculated by VIRIDIC (**b**). Authentic species of *Kayvirus* as per ICTV listing are shown in italics. ¶unclassified; *authentic species of *Kayvirus*.

from patients' wound infections. This is the first description of a wildlife-associated staphylococcal phage capable of eliminating target bacteria before its replication, preventing the formation of phage-resistant mutants. Obligate lytic attributes, broad host (*S. aureus*) range and the absence of virulence/drug-resistant genes in RuSa1 warrants further testing of the present phage in therapeutics of MRSA infections.

Data availability

The DDBJ/ENA/GenBank accession number for the complete genome sequence of RuSa1 is OQ434248.

Received: 22 June 2024; Accepted: 25 February 2025
Published online: 01 March 2025

References

1. Verhoeven, P. O. et al. Detection and clinical relevance of *Staphylococcus aureus* nasal carriage: An update. *Expert Rev. Anti. Infect. Ther.* **12**, 75–89. https://doi.org/10.1586/14787210.2014.859985 (2014).
2. Unnikrishnan, R., Anjana, R. M. & Mohan, V. Diabetes mellitus and its complications in India. *Nat. Rev. Endocrinol.* **12**, 357–370. https://doi.org/10.1038/nrendo.2016.53 (2016).
3. Pauli, N. T. et al. *Staphylococcus aureus* infection induces protein A-mediated immune evasion in humans. *J. Exp. Med.* **211**, 2331–2339. https://doi.org/10.1084/jem.20141404 (2014).
4. World Health Organization, *WHO global strategy for containment of antimicrobial resistance*, (2001).
5. Chhibber, S., Kaur, J. & Kaur, S. Liposome entrapment of bacteriophages improves wound healing in a diabetic mouse MRSA infection. *Front. Microbiol.* **9**, 561. https://doi.org/10.3389/fmicb.2018.00561 (2018).
6. Enright, M. C. et al. The evolutionary history of methicillin-resistant *Staphylococcus aureus* (MRSA). *Proc. Natl. Acad. Sci. USA* **99**, 7687–7692. https://doi.org/10.1073/pnas.122108599 (2002).
7. Horne, K. C. et al. Prospective comparison of the clinical impacts of heterogeneous vancomycin-intermediate methicillin-resistant *Staphylococcus aureus* (MRSA) and vancomycin-susceptible MRSA. *Antimicrob. Agents Chemother.* **53**, 3447–3452. https://doi.org/10.1128/AAC.01365-08 (2009).
8. Pasberg-Gauhl, C. A need for new generation antibiotics against MRSA resistant bacteria. *Drug Discov. Today Technol.* **11**, 109–116. https://doi.org/10.1016/j.ddtec.2014.04.001 (2014).
9. Huon, J. F. et al. Phages versus antibiotics to treat infected diabetic wounds in a mouse model: A microbiological and microbiotic evaluation. *mSystems* **5**, e00542-e520. https://doi.org/10.1128/mSystems.00542-20 (2020).
10. Summers, W. C. Felix Hubert d'Herelle (1873–1949): History of a scientific mind. *Bacteriophage* **6**, e1270090. https://doi.org/10.1080/21597081.2016.1270090 (2016).
11. Petrovic Fabijan, A. et al. Safety of bacteriophage therapy in severe *Staphylococcus aureus* infection. *Nat. Microbiol.* **5**, 465–472. https://doi.org/10.1038/s41564-019-0634-z (2020).
12. Pallavali, R. R., Degati, V. L., Lomada, D., Reddy, M. C. & Durbaka, V. R. P. Isolation and *in vitro* evaluation of bacteriophages against MDR-bacterial isolates from septic wound infections. *PLoS One* **12**, e0179245. https://doi.org/10.1371/journal.pone.0179245 (2017).
13. Ji, J. et al. Identification of a novel phage targeting methicillin-resistant *Staphylococcus aureus In vitro* and *In vivo*. *Microb. Pathog.* **149**, 104317. https://doi.org/10.1016/j.micpath.2020.104317 (2020).
14. Nasser, A. et al. Specification of bacteriophage isolated against clinical methicillin-resistant *Staphylococcus aureus*. *Osong. Public Health Res. Perspect* **10**, 20–24. https://doi.org/10.24171/j.phrp.2019.10.1.05 (2019).
15. Pertics, B. Z. et al. Isolation of a novel lytic bacteriophage against a nosocomial methicillin-resistant *Staphylococcus aureus* belonging to ST45. *Biomed. Res. Int.* **2020**, 5463801. https://doi.org/10.1155/2020/5463801 (2020).
16. Barros, J. et al. Lytic bacteriophages against multidrug-resistant *Staphylococcus aureus, Enterococcus faecalis* and *Escherichia coli* isolates from orthopaedic implant-associated infections. *Int. J. Antimicrob. Agents* **54**, 329–337. https://doi.org/10.1016/j.ijantimicag.2019.06.007 (2019).
17. Shetru, M. N., Karched, M. & Agsar, D. Locally isolated broad host-range bacteriophage kills methicillin-resistant *Staphylococcus aureus* in an *in vivo* skin excisional wound model in mice. *Microb. Pathog.* **152**, 104744. https://doi.org/10.1016/j.micpath.2021.104744 (2021).
18. Gupta, P., Singh, H. S., Shukla, V. K., Nath, G. & Bhartiya, S. K. Bacteriophage therapy of chronic nonhealing wound: Clinical study. *Int. J. Low Extrem. Wounds* **18**, 171–175. https://doi.org/10.1177/1534734619835115 (2019).
19. Patel, D. R., Bhartiya, S. K., Kumar, R., Shukla, V. K. & Nath, G. Use of customized bacteriophages in the treatment of chronic nonhealing wounds: A prospective study. *Int. J. Low Extrem. Wounds* **20**, 37–46. https://doi.org/10.1177/1534734619881076 (2021).
20. Cerveny, K. E., DePaola, A., Duckworth, D. H. & Gulig, P. A. Phage therapy of local and systemic disease caused by *Vibrio vulnificus* in iron-dextran-treated mice. *Infect. Immun.* **70**, 6251–6262. https://doi.org/10.1128/IAI.70.11.6251-6262.2002 (2002).
21. Kutter, E. Phage host range and efficiency of plating. *Methods Mol. Biol.* **501**, 141–149. https://doi.org/10.1007/978-1-60327-164-6_14 (2009).
22. Kropinski, A. M., Mazzocco, A., Waddell, T. E., Lingohr, E. & Johnson, R. P. Enumeration of bacteriophages by double agar overlay plaque assay. *Methods Mol. Biol.* **501**, 69–76. https://doi.org/10.1007/978-1-60327-164-6_7 (2009).
23. Bonilla, N. et al. Phage on tap-a quick and efficient protocol for the preparation of bacteriophage laboratory stocks. *PeerJ* **4**, e2261. https://doi.org/10.7717/peerj.2261 (2016).
24. Kauffman, K. M. & Polz, M. F. Streamlining standard bacteriophage methods for higher throughput. *MethodsX* **5**, 159–172. https://doi.org/10.1016/j.mex.2018.01.007 (2018).
25. Yang, H., Liang, L., Lin, S. & Jia, S. Isolation and characterization of a virulent bacteriophage AB1 of *Acinetobacter baumannii*. *BMC Microbiol.* **10**, 131. https://doi.org/10.1186/1471-2180-10-131 (2010).
26. Kropinski, A. M. Practical advice on the one-step growth curve. *Methods Mol. Biol.* **1681**, 41–47. https://doi.org/10.1007/978-1-4939-7343-9_3 (2018).
27. Hyman, P. & Abedon, S. T. Practical methods for determining phage growth parameters. *Methods Mol. Biol.* **501**, 175–202. https://doi.org/10.1007/978-1-60327-164-6_18 (2009).
28. Lehman, S. M. et al. Design and preclinical development of a phage product for the treatment of antibiotic-resistant *Staphylococcus aureus* infections. *Viruses* **11**, 88. https://doi.org/10.3390/v11010088 (2019).
29. Chen, L. et al. *In vitro* design and evaluation of phage cocktails against *Aeromonas salmonicida*. *Front. Microbiol.* **9**, 1476. https://doi.org/10.3389/fmicb.2018.01476 (2018).
30. Vipin, C. et al. Potential synergistic activity of quercetin with antibiotics against multidrug-resistant clinical strains of *Pseudomonas aeruginosa*. *PLoS One* **15**, e0241304. https://doi.org/10.1371/journal.pone.0241304 (2020).
31. Stepanovic, S., Vukovic, D., Dakic, I., Savic, B. & Svabic-Vlahovic, M. A modified microtiter-plate test for quantification of staphylococcal biofilm formation. *J. Microbiol. Methods* **40**, 175–179. https://doi.org/10.1016/s0167-7012(00)00122-6 (2000).

32. Suchithra, K. V., Hameed, A., Rekha, P. D. & Arun, A. B. Description and host-range determination of phage PseuPha1, a new species of *Pakpunavirus* infecting multidrug-resistant clinical strains of *Pseudomonas aeruginosa*. *Virology* **585**, 222–231. https://doi.org/10.1016/j.virol.2023.06.009 (2023).
33. Kabwe, M. et al. Novel bacteriophages capable of disrupting biofilms from clinical strains of *Aeromonas hydrophila*. *Front. Microbiol.* **11**, 194. https://doi.org/10.3389/fmicb.2020.00194 (2020).
34. Cheng, H. R. & Jiang, N. Extremely rapid extraction of DNA from bacteria and yeasts. *Biotechnol. Lett.* **28**, 55–59. https://doi.org/10.1007/s10529-005-4688-z (2006).
35. Bilung, L. M., Pui, C. F., Su'ut, L. & Apun, K. Evaluation of BOX-PCR and ERIC-PCR as molecular typing tools for pathogenic *Leptospira*. *Dis. Markers* **2018**, 1351634. https://doi.org/10.1155/2018/1351634 (2018).
36. Pavel, A. B. & Vasile, C. I. PyElph - A software tool for gel images analysis and phylogenetics. *BMC Bioinform.* **13**, 9. https://doi.org/10.1186/1471-2105-13-9 (2012).
37. Altamirano, F. L. G. & Barr, J. J. Screening for lysogen activity in therapeutically relevant bacteriophages. *Bio Protoc.* **11**, e3997. https://doi.org/10.21769/BioProtoc.3997 (2021).
38. Menon, N. D. et al. A novel N4-Like bacteriophage isolated from a wastewater source in south india with activity against several multidrug-resistant clinical *Pseudomonas aeruginosa* isolates. *mSphere* **6**, 1128. https://doi.org/10.1128/mSphere.01215-20 (2021).
39. Bankevich, A. et al. SPAdes: A new genome assembly algorithm and its applications to single-cell sequencing. *J. Comput. Biol.* **19**, 455–477. https://doi.org/10.1089/cmb.2012.0021 (2012).
40. Gurevich, A., Saveliev, V., Vyahhi, N. & Tesler, G. QUAST: Quality assessment tool for genome assemblies. *Bioinformatics* **29**, 1072–1075. https://doi.org/10.1093/bioinformatics/btt086 (2013).
41. Olson, R. D. et al. Introducing the bacterial and viral bioinformatics resource center (BV-BRC): A resource combining PATRIC IRD and ViPR. *Nucleic Acids Res.* **51**, D678–D689. https://doi.org/10.1093/nar/gkac1003 (2023).
42. Zimmermann, L. et al. A completely reimplemented MPI bioinformatics toolkit with a new HHpred server at its core. *J. Mol. Biol.* **430**, 2237–2243. https://doi.org/10.1016/j.jmb.2017.12.007 (2018).
43. Grant, J. R. et al. Proksee: In-depth characterization and visualization of bacterial genomes. *Nucleic Acids Res.* **51**, W484–W492. https://doi.org/10.1093/nar/gkad326 (2023).
44. Altschul, S. F., Gish, W., Miller, W., Myers, E. W. & Lipman, D. J. Basic local alignment search tool. *J. Mol. Biol.* **215**, 403–410. https://doi.org/10.1016/S0022-2836(05)80360-2 (1990).
45. Moraru, C., Varsani, A. & Kropinski, A. M. VIRIDIC-A novel tool to calculate the intergenomic similarities of prokaryote-infecting viruses. *Viruses* **12**, 1268. https://doi.org/10.3390/v12111268 (2020).
46. Thompson, J. D., Gibson, T. J., Plewniak, F., Jeanmougin, F. & Higgins, D. G. The CLUSTAL_X windows interface: Flexible strategies for multiple sequence alignment aided by quality analysis tools. *Nucleic Acids Res.* **25**, 4876–4882. https://doi.org/10.1093/nar/25.24.4876 (1997).
47. Tamura, K. et al. MEGA5: Molecular evolutionary genetics analysis using maximum likelihood, evolutionary distance, and maximum parsimony methods. *Mol. Biol. Evol.* **28**, 2731–2739. https://doi.org/10.1093/molbev/msr121 (2011).
48. Tamura, K. & Nei, M. Estimation of the number of nucleotide substitutions in the control region of mitochondrial DNA in humans and chimpanzees. *Mol. Biol. Evol.* **10**, 512–526. https://doi.org/10.1093/oxfordjournals.molbev.a040023 (1993).
49. Felsenstein, J. Confidence limits on phylogenies: An approach using the bootstrap. *Evolution* **39**, 783–791. https://doi.org/10.1111/j.1558-5646.1985.tb00420.x (1985).
50. Jiang, Y., Xu, Q., Jiang, L. & Zheng, R. Isolation and characterization of a lytic *Staphylococcus aureus* phage WV against *Staphylococcus aureus* biofilm. *Intervirology* **64**, 169–177. https://doi.org/10.1159/000515282 (2021).
51. Li, L. & Zhang, Z. Isolation and characterization of a virulent bacteriophage SPW specific for *Staphylococcus aureus* isolated from bovine mastitis of lactating dairy cattle. *Mol. Biol. Rep.* **41**, 5829–5838. https://doi.org/10.1007/s11033-014-3457-2 (2014).
52. D'Souza, R. et al. Complete genome sequence of *Staphylococcus aureus* phage SA75, isolated from goat feces. *Microbiol. Resour. Announc.* **9**, 10–1128. https://doi.org/10.1128/MRA.00114-20 (2020).
53. Jurczak-Kurek, A. et al. Biodiversity of bacteriophages: Morphological and biological properties of a large group of phages isolated from urban sewage. *Sci. Rep.* **6**, 34338. https://doi.org/10.1038/srep34338 (2016).
54. Oduor, J. M. O., Kadija, E., Nyachieo, A., Mureithi, M. W. & Skurnik, M. Bioprospecting *Staphylococcus* phages with therapeutic and bio-control potential. *Viruses* **12**, 133. https://doi.org/10.3390/v12020133 (2020).
55. Kazmierczak, N., Grygorcewicz, B., Roszak, M., Bochentyn, B. & Piechowicz, L. Comparative assessment of bacteriophage and antibiotic activity against multidrug-resistant *Staphylococcus aureus* biofilms. *Int. J. Mol. Sci.* **23**, 1274. https://doi.org/10.3390/ijms23031274 (2022).
56. Mato, R. et al. Spread of the multiresistant Iberian clone of methicillin-resistant *Staphylococcus aureus* (MRSA) to Italy and Scotland. *Microb. Drug. Resist.* **4**, 107–112. https://doi.org/10.1089/mdr.1998.4.107 (1998).
57. Monecke, S. et al. A field guide to pandemic, epidemic and sporadic clones of methicillin-resistant *Staphylococcus aureus*. *PLoS One* **6**, e17936. https://doi.org/10.1371/journal.pone.0017936 (2011).
58. Principi, N., Silvestri, E. & Esposito, S. Advantages and limitations of bacteriophages for the treatment of bacterial infections. *Front. Pharmacol.* **10**, 513. https://doi.org/10.3389/fphar.2019.00513 (2019).
59. Koskella, B. & Meaden, S. Understanding bacteriophage specificity in natural microbial communities. *Viruses* **5**, 806–823. https://doi.org/10.3390/v5030806 (2013).
60. Ross, A., Ward, S. & Hyman, P. More Is better: Selecting for broad host range bacteriophages. *Front. Microbiol.* **7**, 1352. https://doi.org/10.3389/fmicb.2016.01352 (2016).
61. Sergueev, K. V. et al. Correlation of host range expansion of therapeutic bacteriophage Sb-1 with allele state at a hypervariable repeat locus. *Appl. Environ. Microbiol.* **85**, e01209-e1219. https://doi.org/10.1128/AEM.01209-19 (2019).
62. Leskinen, K. et al. Characterization of vB_SauM-fRuSau02, a Twort-Like bacteriophage isolated from a therapeutic phage cocktail. *Viruses* **9**, 258. https://doi.org/10.3390/v9090258 (2017).
63. Oduor, J. M. O. et al. Genomic characterization of four novel *Staphylococcus myoviruses*. *Arch. Virol.* **164**, 2171–2173. https://doi.org/10.1007/s00705-019-04267-0 (2019).
64. Walker, P. J. et al. Changes to virus taxonomy and to the International code of virus classification and nomenclature ratified by the international committee on taxonomy of viruses (2021). *Arch. Virol.* **166**, 2633–2648. https://doi.org/10.1007/s00705-021-05156-1 (2021).
65. Garcia-Vallvé, S., Palau, J. & Romeu, A. Horizontal gene transfer in glycosyl hydrolases inferred from codon usage in *Escherichia coli* and *Bacillus subtilis*. *Mol. Biol. Evol.* **16**, 1125–1134. https://doi.org/10.1093/oxfordjournals.molbev.a026203 (1999).

Acknowledgements

The authors acknowledge anonymous reviewers for their constructive comments on this manuscript. We would like to thank Mr. H Jayaprakash Bhandary, Director and Jerald Vikram Lobo, Scientific Officer, Pilikula Biological Park for providing access to the wastewater samples. The authors express gratitude to Dr. Sebanti Gupta for kindly gifting *S. aureus* ATCC BAA-44, Mr. Yuvarajan Subramanian for fluorescence microscopy and Dr. Vijayakumar Hiremath for transmission electron microscopy. KVS thanks the staff of Central Laboratory, Yenepoya Medical College Hospital for kindly providing the clinical isolates. KVS and ABA acknowledge Yenepoya

(Deemed to be University) for a JRF fellowship and Seed Grant (YU/seed grant/127-2022), respectively.

Author contributions

Conceptualization: ABA and AH; methodology: KVS and AH; validation, KVS, AH and PS; investigation, KVS and AH; resources, ABA and PDR; data curation, KVS, AH and PS; writing-original draft preparation, KVS; writing-review and editing, AH, ABA and PDR; visualization, KVS, AH and PS; supervision, ABA and AH; project administration, ABA; All authors have read and agreed to the published version of the manuscript.

Declarations

Competing interests

The authors declare no competing interests.

Ethical approval

This study was approved by the Institutional Ethics Committee (IEC), Yenepoya Medical College (Protocol number YEC-1/2022/132). All methods performed in this study were in accordance with the relevant guidelines and regulations drafted by IEC. MRSA isolates originated from infected wounds from patients admitted to YMCH obtained from the Central Microbiology Laboratory, Yenepoya. Samples were collected for a period of six months.

Additional information

Supplementary Information The online version contains supplementary material available at https://doi.org/10.1038/s41598-025-92032-6.

Correspondence and requests for materials should be addressed to A.H. or A.B.A.

Reprints and permissions information is available at www.nature.com/reprints.

Publisher's note Springer Nature remains neutral with regard to jurisdictional claims in published maps and institutional affiliations.